Coincident proton emission induced by 200 MeV protons on ^{197}Au

S. V. Förtsch
National Accelerator Centre, P.O. Box 72, Faure, 7131, South Africa

A. A. Cowley
Department of Physics, University of Stellenbosch, Stellenbosch, 7600, South Africa

J. J. Lawrie, J. V. Pilcher, F. D. Smit, and D. M. Whittal
National Accelerator Centre, P.O. Box 72, Faure, 7131, South Africa
(Received 30 March 1993)

Coincident cross sections were measured for the reaction ^{197}Au$(p,p'p'')$ at an incident energy of 200 MeV. The protons emitted from the continuum were detected at primary laboratory angles of $-40°$, $-50°$, and $-60°$, for secondary angles ranging between 20° and 150°. The theoretical model which was used to interpret the coincident spectra describes the reaction mechanism in terms of a quasifree nucleon-nucleon interaction between the projectile and a bound target nucleon, folded with a probability for emission of the quasifree knocked-on nucleon after inelastic rescattering off the residual target nucleus. The validity of the distorted-wave impulse approximation which describes the initial quasifree interaction was confirmed by measuring the quasifree knockout of valence-orbital protons from ^{197}Au. The measured coincident continuum cross sections were then compared with model calculations for primary proton energy cuts around 90, 70, and 40 MeV. The reasonable agreement found between the calculated and measured cross sections indicates that the signature of quasifree scattering persists in the continuum emission from a nucleus as heavy as ^{197}Au, and is not obscured by multiple scattering effects.

PACS number(s): 24.10.−i, 25.40.−h

I. INTRODUCTION

During the mid-1960s it was discovered that a preequilibrium reaction mechanism plays an important role in the interaction of energetic nuclear projectiles with atomic nuclei. Subsequently considerable progress has been made towards an understanding of the underlying physics, leading to a satisfactory formulation of the quantum-mechanical multistep theory [1]. These theoretical advances originated from numerous experiments which explored mostly inclusive reactions. A small number of measurements of coincident-particle emission from excitations corresponding to the preequilibrium process are also available, but the required theoretical formulation still needs to be developed to the same degree of sophistication as that which applies to the modeling of inclusive data.

Analyses of experimental data obtained for inclusive reactions indicate that the description of the interaction in terms of successive statistical multistep nucleon-nucleon collisions appears to be sound. Furthermore, the coincidence type of experiment suggests that the initial nucleon-nucleon interaction can be viewed as a quasifree interaction and that the two nucleons then act as intranuclear projectiles which generally undergo further interactions as they traverse the nucleus. Thus, by varying the kinematic conditions appropriately, the expected frequency of subsequent collisions can be adjusted in the coincidence experiments to lead to characteristic features in the observed angular correlations. This was investigated by Cowley *et al.* [2] and Ciangaru *et al.* [3] for ^{58}Ni at 100 and 200 MeV, respectively.

The theoretical analysis developed by Ciangaru [4] is based on the same general ideas as those of Feshbach, Kerman, and Koonin [5], which find wide application in the description of inclusive reactions. However, in previous applications of the Ciangaru theory, simplifications have been introduced to make calculations tractable, and the validity of some of these is more easily judged for a light target nucleus such as ^{12}C, which was studied extensively by Pilcher *et al.* [6].

The present work is an investigation of the reaction ^{197}Au$(p,p'p'')$ at an incident energy of 200 MeV, and was performed to determine whether the ideas regarding the reaction mechanism extracted from earlier experiments on ^{12}C [6] and ^{58}Ni [2, 3] also extrapolate to a heavy target nucleus. Some of the results presented in this paper have been published [7], but considerably more experimental data are now available, together with a more refined analysis. As expected, this work confirms our earlier conclusions, and the expanded analysis allows us to present quantitative information on various aspects of the reaction.

For the purpose of comparison with theory, the experimental data are divided into two groups according to the most likely reaction mechanism for each set. Data corresponding to a missing mass of less than 10 MeV would not be expected to involve an appreciable degree of inelastic rescattering during the process of quasifree knockout. Therefore, energy sharing spectra are generated for these data; the reaction is treated as a purely quasifree knockout and is denoted as ^{197}Au$(p,2p)^{196}$Pt.

On the other hand, coincidence data corresponding to a missing mass of greater than 10 MeV are indicated as the reaction ^{197}Au$(p,p'p'')$ to emphasize the theoretical inclusion of inelastic rescattering following the initial quasifree interaction. Thus the selection of ejectile energies and the way in which the cross sections are presented serve to display selectively the features which are most characteristic of the two reaction mechanisms.

The experimental details of the investigation are presented in Sec. II, the theory is summarized in Sec. III, and the calculations are described in Sec. IV. The results, with a discussion of the implications, are given in Sec. V. Finally, in Sec. VI we provide a summary and draw our conclusions.

II. EXPERIMENTAL PROCEDURE

The experiment was performed at the cyclotron facility of the National Accelerator Centre. A detailed description of the layout of the facility and equipment is given in Ref. [6] and references therein.

The energy of the extracted proton beam was 200 ± 1.0 MeV. The estimated energy spread of about 100 keV was negligible compared with the 1 MeV energy resolution of the NaI detectors used in the experiment. The beam was focused to a spot size of less than 2×2 mm at the target center of a 1.5 m diameter scattering chamber.

The target was a high-purity (99.9%) gold foil of thickness 4.02 ± 0.10 mg/cm^2 and with a uniformity of better than 0.5%/mm. Four double-element detector telescopes were mounted in the same horizontal reaction plane on stands bolted onto two movable arms in the scattering chamber. The coplanar configuration of the detector setup consisted of one "primary" detector telescope ($T1$) and three "secondary" detector telescopes ($T2$–$T4$) on the opposite side of the beam as illustrated in Fig. 1. Each detector telescope consisted of a 1000 μm Si surface barrier (ΔE) detector followed by a 76 (diam) $\times$ 127 mm NaI(Tl) stopping (E) detector. Both the primary and the secondary telescope $T2$, which were positioned in the most forward direction with respect to the beam, were equipped with active collimators as described in Ref. [6]. Additionally, all detector telescopes were shielded by 55 mm thick brass collimators (thick enough to stop 200 MeV protons). Solid angles ranged between 1.6 and 1.8 msr. The angles between telescopes $T2$ and $T3$, and between telescopes $T3$ and $T4$, were $50.00° \pm 0.05°$. To reduce the incident flux on the surface barrier detectors of low-energy electrons from the target, 8 μm thick Kapton foils were placed over the front holes of the brass collimators.

The linear and fast timing signals were processed with standard fast coincidence electronics. An on-line computer system enabled event-by-event data processing and storage for subsequent off-line analysis. Conventional ΔE-E techniques were applied for charged particle identification.

Energy calibrations of the four Si detectors were carried out with collimated alphas obtained from a ^{228}Th source. The NaI detectors were calibrated according to the kinematics for the elastic scattering of protons from

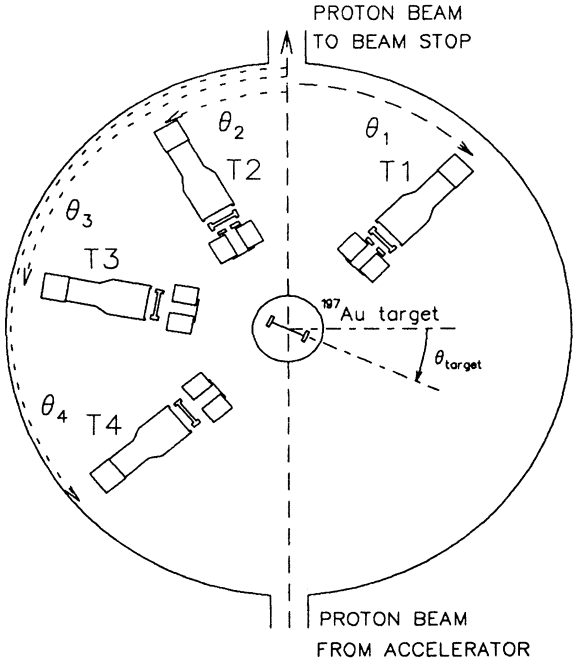

FIG. 1. Coplanar target and detector geometry inside the scattering chamber.

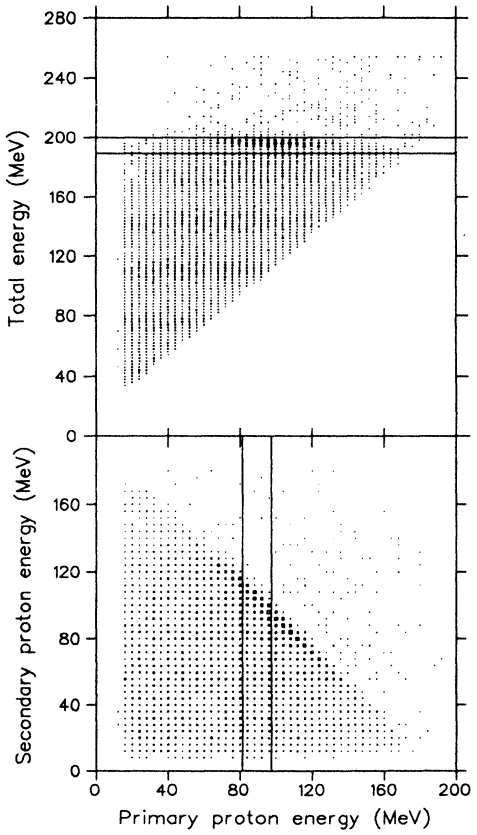

FIG. 2. A typical two-dimensional summed-energy spectrum (above) and energy-sharing spectrum (below) showing coincidence events. The quasifree knockout locus is visible in both plots. Selected regions of the spectra are specified by gates as indicated and are projected onto the energy axis of the primary and secondary proton as described in the text.

TABLE I. Sets of primary θ_P and secondary θ_S coincidence angles.

θ_P	θ_S
−40°	20°, 40°, 70°, 90°, 120°, 140°
−50°	50°, 100°, 150°
−60°	60°

carbon and hydrogen in a thin polythene target. The beam direction was determined to within 0.1° by measuring elastic cross sections of scattered protons from a carbon target at forward angles on both sides of the beam. Possible gain drifts in the photomultiplier tubes of the NaI detectors were corrected by monitoring a LED pulser system, which also enabled corrections for electronic dead time to be made.

The correction for the NaI detector efficiency was based on the empirical formula of Green *et al.* [8] and differs by about 5% from values for the reaction tail obtained by Measday *et al.* [9] and from those quoted in the Janni tables [10] for 200 MeV protons in NaI. To correct for contributions from random coincidences in the prompt coincidence time peak, integrated events in one purely random peak in the measured coincidence time distribution were subtracted from the events in the prompt time peak.

Coincident energy spectra were extracted from two-dimensional energy histograms. An example of a two-dimensional summed-energy spectrum and the corresponding energy-sharing spectrum are shown in Fig. 2. Also indicated are the gated regions selected to obtain spectra of projections onto the energy axis of the primary and secondary proton, respectively. The primary θ_P and secondary θ_S angles at which data were collected are summarized in Table I.

If it is assumed that all systematic uncertainties are uncorrelated, an estimate of the total systematic error is less than 10%. Important contributions to the experimental systematic error are as follows. The uncertainty in the thickness of the ^{197}Au target is approximately 3%. The solid angle is assumed to be accurate to within 1%. The overall energy uncertainty over the entire range results in a combined uncertainty of about 4% in the absolute cross sections. Further uncertainties are introduced by the setting of particle identification gates and timing gates. Together with an uncertainty in the correction for NaI crystal losses, the total error in the particle identification procedure is estimated to be less than 5%. The systematic error introduced by the subtraction of random coincidence events is less than 3%. Estimated uncertainties due to the beam current integrator, due to electronic dead time, and due to contributions to the relevant regions of the two-dimensional energy histograms from slit scattering off collimators, are estimated to be less than 2%.

III. THEORY

The theoretical analysis is based on the assumption that the formation of continuum spectra is initiated by a quasifree interaction between the projectile and a bound target nucleon resulting in two energetic particles. This process is then further treated as a doorway process for continuum emission through multiple scatterings.

A. DWIA analysis

The cross sections for the initial quasifree knockout interaction were calculated with the computer code THREEDEE [11], which is based on the distorted-wave impulse approximation (DWIA) formalism as described by Chant and Roos [12]. As details of the specific aspects in the DWIA theory which are used in the present calculations are discussed elsewhere [12–14] , we shall present only a brief summary of the theory here.

The calculations which are performed with this model are based on the general expression for a knockout reaction $A(a,cd)B$ where $A = B + b$ and c is the quasifree-scattered projectile a after an interaction with the bound particle b, which is emitted from the target nucleus as particle d.

The triple differential cross section for such a reaction can be expressed as [14]

$$\frac{d^3\sigma}{d\Omega_c d\Omega_d dE_c} = C^2S\,K \sum_{\rho_a\rho_c'\rho_d'' JM} \frac{1}{(2J_A+1)} \frac{1}{(2S_a+1)} \Bigg| \sum_{\sigma_a\sigma_c\sigma_c'\sigma_d\sigma_d''\sigma_b\Lambda} (2L+1)^{\frac{1}{2}} (L\Lambda S_b\sigma_b|JM)\, D^{\frac{1}{2}*}_{\sigma_c\sigma_c'}(R_{ac})\, D^{\frac{1}{2}*}_{\sigma_d\sigma_d''}(R_{ad}) \times T^{L\Lambda}_{\sigma_a\sigma_c'\sigma_d''\rho_a\rho_c'\rho_d''} \langle\sigma_c\sigma_d|t|\sigma_a\sigma_b\rangle \Bigg|^2 , \quad (1)$$

where C^2S is the spectroscopic factor for the final state in B, L is the relative angular momentum of b and B (projection Λ), J_A is the angular momentum of the target [12], J is the angular momentum (projection M) of particle b, S_i are the spin quantum numbers with projections ρ_i and σ_i for particles $i = a, b, c, d$ (as defined by Chant and Roos [14]), and t is the two-body operator for the free N-N scattering process as obtained from the impulse approximation. The primes denote the relative directions of propagation of particles a, c, and d which are defined as follows: the unprimed $\tilde{z}$ axis is along the beam direction while particles c and d propagate parallel to the $\tilde{z}'$ and $\tilde{z}''$ axes, respectively. K is a kinematic factor and $D^{\frac{1}{2}}_{mn}$ are rotation matrices which describe the transformation of spin projections from n to m through

a rotation R_{ai} of the respective set of axes for particle i, into the reference set of axes of the beam direction defined by particle a.

Due to the binding energy of the struck nucleon, the two-body t-matrix is half off shell [15]. Chant and Roos [12] approximate the t matrix by interpolating on-shell N-N phase shifts for two different prescriptions [15] of the total center-of-mass energy $E_{\text{c.m.}}$. In the final energy prescription (FEP), $E_{\text{c.m.}}$ is the relative center-of-mass energy of the emitted particles c and d in the exit channel, whereas the initial energy prescription (IEP) requires selection of the relative center-of-mass energy $E_{\text{c.m.}}$ of the incident particle a and the struck particle b in the entrance channel. The scattering angle is the same in both prescriptions. Although it has been demonstrated that off-shell effects have no severe influence on qualitative characteristics of cross sections at incident energies above 100 MeV, these effects become more important at lower energies [16–18].

B. Coincident continuum emission model

In order to study the mechanism of the coincident proton emission from ^{197}Au we chose two distinct regions in the two-dimensional preequilibrium energy spectrum as displayed in Fig. 2. One region corresponds to protons which are mostly knocked out without undergoing further explicit rescattering from the residual part of the target nucleus. These measured quasifree (QF) particles carry energies which are determined by the energy conservation condition corresponding to the initial knockout interaction of bound valence protons from the $^{197}\text{Au}(p,2p)^{196}\text{Pt}$ reaction. Below the quasifree region lies the major part of the reaction strength. We assume that this second region contains coincident particles which have lost some of their energy mainly through inelastic rescattering off the residual nucleus after the primary knockout collision, also referred to as the "doorway" stage. Although these effects would be included in a distorted-wave analysis by means of the imaginary part of the optical potential for the outgoing particles, such a prescription does not give a full account of the preequilibrium part of the spectrum.

Ciangaru [4] has thus proposed a three-body approach to the multiple scattering direct reactions which lead to continuum spectra. The physical ideas behind this approach are extensively discussed elsewhere [3, 4]. The validity of the model has recently been demonstrated in the interpretation of the $^{12}\text{C}(p,p'p'')$ reaction induced by 200 MeV protons with a refined version of the model [6, 19]. Except for some minor differences in the unfolded components of the total continuum emission cross section which will be discussed later, the model used in the present study is essentially the same as applied by Pilcher *et al.* [6].

A schematic representation of the model is given in Fig. 3. A projectile p_a with energy E_a undergoes a quasifree collision with a bound nucleon inside the target nucleus and is detected as $p_{a'}$ with energy $E_{a'}$ and at a scattering angle $\theta_{a'}$ with respect to the beam direction.

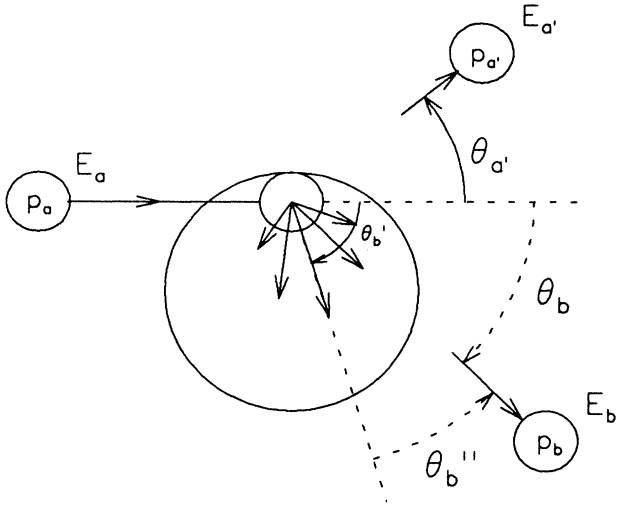

FIG. 3. Schematic illustration of the reaction mechanism for proton continuum spectra from $^{197}\text{Au}(p_a, p_{a'} p_b)$. The energy dissipation of the projectile p_a is studied by means of the protons $p_{a'}$ and p_b which are detected in coincidence and their energies are measured as $E_{a'}$ and E_b at the scattering angles $\theta_{a'}$ and θ_b, respectively. Details in text.

As a result of the collision, the bound nucleon recoils at an angle θ'_b and carries an energy E'_b. It undergoes further interaction with the residual nucleus and eventually the secondary proton p_b is detected in coincidence with the primary proton $p_{a'}$ at an angle θ_b and with energy E_b. A convenient additional simplification to the model, as pointed out by Pilcher *et al.* [6], is that the incident proton p_a is detected as $p_{a'}$ after an initial quasifree collision without any further interaction. This assumption can be considered to be reasonable if the scattering angle $\theta_{a'}$ is in a forward direction with respect to the beam direction. Furthermore, a relatively high energy $E_{a'}$ would minimize any further scattering probabilities of $p_{a'}$.

It is furthermore assumed that the multiple scattering process which the struck quasifree particle p'_b initiates is replaced with a probability for scattering the particle through an angle $\theta''_b = \theta_b - \theta'_b$ in order to detect it as p_b with energy E_b at an angle θ_b. Different assumptions were made previously to express the total inelastic scattering probability. Ciangaru *et al.* [3] scaled it to the total inclusive preequilibrium cross section for inelastic scattering off the residual nucleus. However, in the present study we substitute the total inelastic cross section with the reaction cross section $\sigma_R(E'_b)$, as previously suggested by Pilcher *et al.* [6]. By using the reaction cross section, we argue that all reaction channels of the nucleon-induced reaction should be included in the integrated yield. The probability for inelastic scattering is therefore interpreted as a fraction of all the possible inclusive reaction strength.

The coincident continuum cross section for the reaction $(a, a'b)$ is then written as [6]:

$$\frac{d^4\sigma\left(\theta_{a'}E_{a'}\theta_bE_b\right)}{d\Omega_{a'}d\Omega_b dE_{a'}dE_b}=\int d\theta_b'\sin\theta_b'\sum_\lambda\frac{d^3\sigma_{\lambda\alpha}^{\mathrm{QF}}\left(\theta_{a'}E_{a'}\theta_b'E_b'\right)}{d\Omega_{a'}d\Omega_b'dE_{a'}}\frac{1}{\sigma_R\left(E_b'\right)}\frac{d^2\sigma^{\mathrm{inel}}\left(\theta_b''E_bE_b'\right)}{d\left(\Omega_b-\Omega_b'\right)dE_b}\ , \tag{2}$$

where the cross section of the initial quasifree interaction,

$$\frac{d^3\sigma_{\lambda\alpha}^{\mathrm{QF}}\left(\theta_{a'}E_{a'}\theta_b'E_b'\right)}{d\Omega_{a'}d\Omega_b'dE_{a'}}\ ,$$

is calculated with distorted waves for the protons p_a and $p_{a'}$ and plane waves for the struck nucleon p_b'. Plane waves are used for the knocked-out nucleons because the distortion that these particles experience is included explicitly in the subsequent multiple scattering which eventually leads to the emission of the secondary proton.

The quasifree cross section is summed over the index λ which represents participating valence states in the target nucleus from which bound nucleons are knocked out, leaving the residual nucleus B in quantum state α.

For events to fall onto the quasifree locus, the energies $E_{a'}$ and E_b' of the quasifree particles $p_{a'}$ and p_b' correspond to values which are determined by energy conservation:

$$E_{a'}+E_b'=E_a+E_\lambda-\epsilon_\alpha-E_B\ , \tag{3}$$

where E_λ is the binding energy of the nucleon which is knocked out of the target orbital corresponding to the index λ, ϵ_α is the excitation energy of the residual nucleus in the quantum state α, and E_B is the recoil energy of the residual nucleus.

Further contributions to the observed yield that were included in Ref. [6] are the knockout of neutrons in the initial step, and an out-of-plane component to the proton continuum. These are refinements to the original model of Ciangaru [4].

By including explicitly the quasifree scattering of both protons and neutrons in and out of plane, the continuum cross section for coincident protons detected in the reaction plane then becomes [6]

$$\frac{d^4\sigma\left(\theta_{a'}E_{a'}\theta_bE_b\right)}{d\Omega_{a'}d\Omega_b dE_{a'}dE_b}=\sum_N\left[\int d\Omega_b'\sum_\lambda\frac{d^3\sigma_{\lambda\alpha}^{\mathrm{QF}}\left(\theta_{a'}E_{a'}\theta_b'E_b'\beta\right)}{d\Omega_{a'}d\Omega_b'dE_{a'}}\frac{1}{\sigma_R\left(E_b'\right)}\frac{d^2\sigma^{\mathrm{inel}}\left(\gamma E_bE_b'\right)}{d\left(\Omega_b-\Omega_b'\right)dE_b}\right]_N\ , \tag{4}$$

where the sum over N indicates the separate evaluations for the initial knockout of protons and neutrons, β is the out-of-plane angle of the knocked-out nucleon, and γ is the angle between the struck nucleon and the secondary proton detected at an angle θ_b. The solid angle element $d\Omega_b'$ of the integration is expressed as [6]

$$d\Omega_b'=\sin\theta_b'\,d\theta_b'\,d\beta\ . \tag{5}$$

The angle γ is defined as

$$\cos\gamma=\cos\beta\cos\left(\theta_b-\theta_b'\right)\ . \tag{6}$$

IV. CALCULATIONS

A. Quasifree knockout

In order to judge whether the DWIA provides an appropriate description of the initial nucleon-nucleon interaction in ^{197}Au, calculations of the quasifree knockout of bound protons were performed for the reaction $^{197}\mathrm{Au}(p,2p)^{196}\mathrm{Pt}$ to discrete final states. These calculations were then compared with experimental energy-sharing distributions extracted from the data for missing-mass values up to 10 MeV. Discrete knockout of valence protons should be energetically favored, but these are not resolved experimentally (see Fig. 2).

The triple differential cross section for a quasifree knockout reaction as expressed in the DWIA by Eq. (1) is calculated by THREEDEE. The distorted waves of the incident proton and the two quasifree scattered protons were generated from spin-dependent optical potentials. In order to test the sensitivity of the DWIA with regard to distorting optical potentials, results with parameters from Nadasen *et al.* [20] were compared with calculations which utilized parameters of Madland [21]. The Madland potential is valid for incident nucleon energies between 50 and 400 MeV, and is derived from the potential of Schwandt *et al.* [22].

The bound-state wave function is the eigenfunction generated by THREEDEE by adjusting the depth of a Woods-Saxon potential to reproduce the given binding energy as the eigenvalue. Representative bound-state parameters were taken from Chant *et al.* [14], viz., radius parameter $R_R = 1.25$ fm, diffuseness $a_R = 0.63$ fm, and spin-orbit well depth $V_{\mathrm{SO}} = 5$ MeV. An average value of 5.8 MeV [23] was taken as the binding energy of a valence proton in ^{197}Au. Relative spectroscopic factors for the

TABLE II. Spectroscopic factors C^2S and binding energies of the valence proton and neutron states in ^{197}Au.

Protons (Binding energy ~ 5.8 MeV)		Neutrons (Binding energy ~ 8.1 MeV)	
State	C^2S	State	C^2S
$1h_{11/2}$	10.3	$1i_{13/2}$	11.2
$3s_{1/2}$	1.6	$1h_{9/2}$	8.0
$2d_{3/2}$	2.6	$2f_{7/2}$	6.4
$2d_{5/2}$	5.4	$1h_{11/2}$	9.6

proton removal from the $2d_{3/2}$, $2d_{5/2}$, and $1h_{11/2}$ states were taken from results obtained by Langevin-Joliot *et al.* [24] for the pickup reaction ^{197}Au$(d,^3$He$)^{196}$Pt. A component from the $3s_{1/2}$ state was included to have the same relative occupation probability as the average of these three states (see Table II).

B. Coincident continuum emission

The cross sections for the initial quasifree interaction

$$\frac{d^3\sigma_{\lambda\alpha}^{\mathrm{QF}}(\theta_{a'}E_{a'}\theta_b'E_b'\beta)}{d\Omega_{a'}d\Omega_b'dE_{a'}}$$

as required in the convolution integral [Eq. (4)], were calculated in a similar way to those for the knockout to discrete states. The distributions of the nucleons which initiate further interactions in the recoiling nucleus are therefore based on the DWIA-predicted cross sections for the ^{197}Au$(p,2p)$ and ^{197}Au(p,pn) reactions. The intranuclear nucleons are described by plane waves, while distorted waves represent the incoming proton and the scattered primary proton. The applicability of the DWIA in calculations of quasifree neutron knockout cross sections has been demonstrated by Watson *et al.* [25] on (p,pn) coincidence data from two Ca isotopes measured at an incident proton energy of 150 MeV.

The neutron knockout distributions are assumed to be dominated by contributions from the four valence neutron states $1i_{13/2}$, $1h_{9/2}$, $2f_{7/2}$, and $1h_{11/2}$ in ^{197}Au. An average binding energy of 8.1 MeV [23] was adopted for the bound neutrons. The respective spectroscopic factors for these states were assumed to be 80% of their sum-rule values which correspond to the average occupation probabilities of the proton states as summarized in Table II. Results for the neutron knockout cross sections with optical-model parameters of Nadasen *et al.* were compared with those obtained with the Madland set. In the case of the Madland potential, the neutron-nucleus potential is obtained by including both a Lane-model assumption and a Coulomb-correction term in the corresponding real central proton potential [21].

The DWIA cross sections obtained with the two different sets of optical potentials differed by 20–30% in the predicted proton and neutron yields. As these differences are not considered to be significant in the context of the emission model, only the distributions based on the Nadasen potentials were used in the complete model calculations.

As a simplification to the model we assume that the relative contributions to the out-of-plane cross sections are related to the distribution at the secondary angle where the calculated coplanar knockout yield reaches a maximum. An out-of-plane quasifree scattering component is thus included in the cross section by simply scaling the in-plane contribution with this relative out-of-plane distribution.

The calculations of the convolution integral given by Eq. (4) were then carried out by substituting the expressions for the quasifree knockout and the inelastic cross section with analytic functions. The angular distributions for the knocked-on nucleon were parametrized by fitting polynomials $f(\theta_b')$ and $k(\beta)$ to the in- and out-of-plane cross sections, respectively. The out-of-plane contribution was taken into account by multiplying the in-plane distribution $f(\theta_b')$ by a dimensionless scaling factor $\frac{k(\beta)}{k(0)}$, where $k(0)$ is the maximum in-plane cross section.

The inelastic scattering cross section of the bound nucleon emerging from the initial quasifree interaction with the residual nucleus,

$$\frac{d^2\sigma^{\mathrm{inel}}(\gamma E_b E_b')}{d(\Omega_b-\Omega_b')dE_b},$$

is described with the phenomenological prescription of Kalbach [26]. These parametrized angular distributions were normalized to the experimental data for the ^{197}Au(p,p') reaction, as described in Ref. [27]. As experimental ^{197}Au(n,p) data are not available in the required incident energy range, absolute normalizations for this reaction were based on angle-integrated (n,p) yields predicted by the geometry-dependent hybrid model code ALICE [28]. Reaction cross sections $\sigma_R(E_b')$ for normalizing the calculated inelastic cross sections were obtained from the parameterization of Silberberg and Tsao [29] for the (p,p') and (n,p) reactions on ^{197}Au.

For the exclusive reaction ^{197}Au$(a,a'b)$, Eq. (4) is then written as

$$\frac{d^4\sigma}{d\Omega_{a'}d\Omega_b dE_{a'}dE_b}=2\kappa\sum_N\left[\frac{\eta(E_b,E_b')}{\sinh[\eta(E_b,E_b')]}\frac{d\sigma^{\mathrm{inel}}(E_b,E_b')}{dE_b}\frac{1}{\sigma_R(E_b')}\right.$$
$$\left.\times\int_0^{2\pi}\int_0^{\pi/2}\cos\beta\frac{k(\beta)}{k(0)}f(\theta_b')\,e^{\eta(E_b,E_b')\cos\beta\cos(\theta_b-\theta_b')}d\beta d\theta_b'\right], \quad (7)$$

where $\eta(E_b,E_b')$ is the modified slope parameter in the Kalbach phenomenological prescription (see Ref. [27]). The angle-integrated cross sections $\frac{d\sigma^{\mathrm{inel}}}{dE_b}$ correspond to the normalizations required for the Kalbach parametrization of the inclusive angular distributions as described above. The factor κ is used to normalize the calculated continuum emission cross sections to the experimental data.

V. RESULTS AND DISCUSSION

A. Results for ^{197}Au$(p,2p)^{196}$Pt

Experimental cross sections as a function of the primary proton energy for the quasifree knockout of protons from unresolved discrete valence states up to a missing mass of 10 MeV are shown in Figs. 4 and 5. In Fig. 4 we

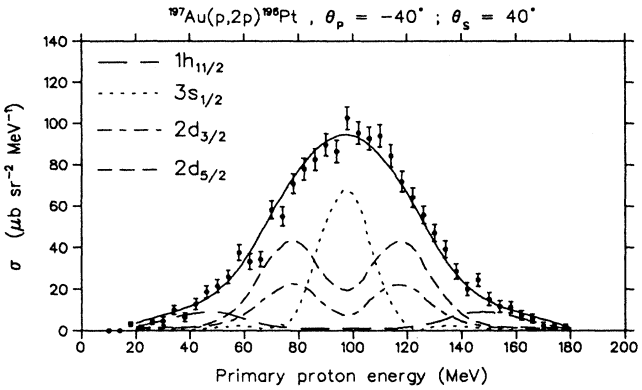

FIG. 4. Energy-sharing cross sections for the knockout of valence-orbital protons up to a missing mass of 10 MeV from ^{197}Au for the primary proton angle θ_P and secondary proton angle θ_S as indicated. Experimental data points are shown with statistical error bars. The curves are DWIA calculations using the final energy prescription (FEP), of the relative contributions from the four valence proton states as indicated, and the sum (solid line). The spectroscopic factors are given in Table II, and an overall normalization factor is listed in Table III.

display the relative contributions to the quasifree knockout cross section from the four valence proton states in ^{197}Au $(1h_{11/2}, 3s_{1/2}, 2d_{3/2}, 2d_{5/2})$, with spectroscopic factors as given in Table II and an overall normalization as listed in Table III, together with the sum of the contributions. The data in Fig. 4 indicate that an occupation

TABLE III. Summary of the primary θ_P and secondary θ_S proton angles for the valence-state knockout calculations of ^{197}Au$(p, 2p)^{196}$Pt with required normalization factors F.

θ_P	θ_S	F
−40°	40°	0.46
−50°	50°	0.4
−60°	60°	0.35
−40°	20°	0.5
−40°	70°	0.5
−40°	90°	0.38

probability for the $3s_{1/2}$ proton state comparable to those of the other states has to be included. This differs from the pickup reaction studies of Langevin-Joliot *et al.* [24] where negligible strength of the $3s_{1/2}$ state was found. Our results nevertheless seem to be reasonable, since at this near-quasifree angle pair (−40°, 40°) the cross section is sensitive to low momentum components of the wave function of the bound proton. It may be argued that due to the large momentum mismatch in the pickup reaction studied by Langevin-Joliot *et al.* [24], that reaction is not a sensitive probe of the $3s_{1/2}$ strength. The effect of changes in the spectroscopic factor of the $3s_{1/2}$ state is found to be less significant at the other angle pairs, as might be expected when larger recoil momenta dominate the cross section.

There is good overall shape agreement between the DWIA calculations and the experimental distributions shown in Fig. 5. The differences between the DWIA cal-

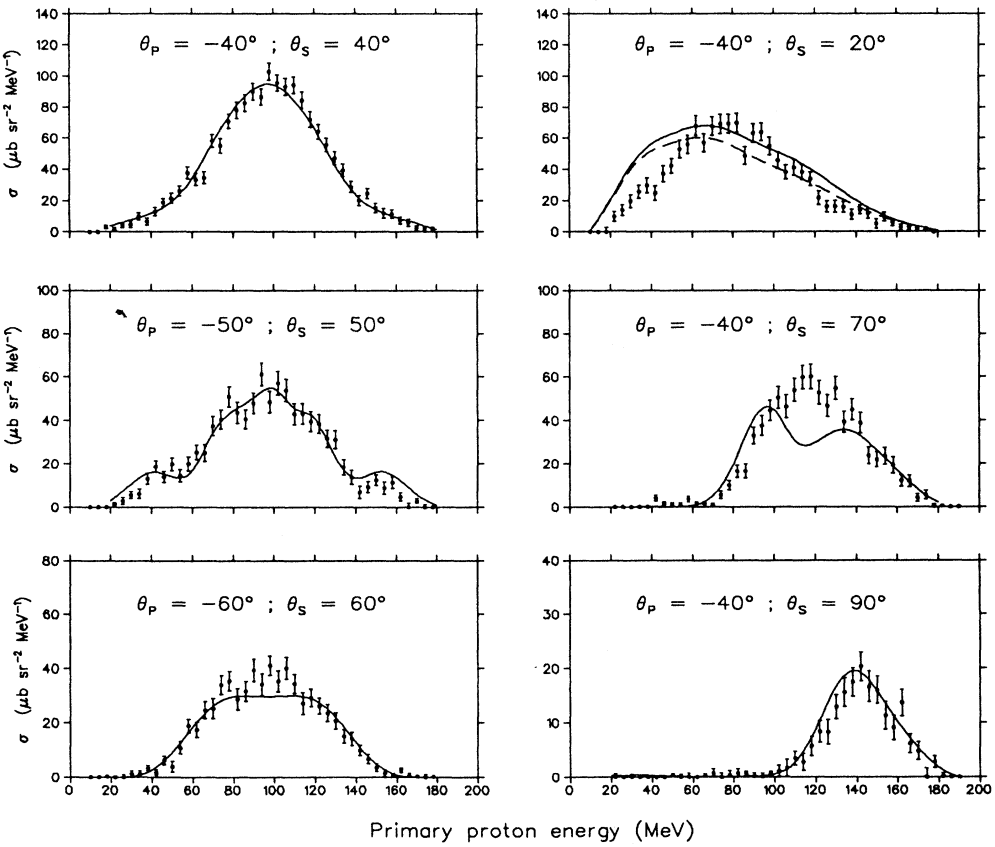

FIG. 5. See caption of Fig. 4. The curves are summed DWIA calculations of relative contributions from the four valence proton states in ^{197}Au performed with the FEP (continuous curve) and, for the (−40°, 20°) angle pair, also with the IEP (dashed curve).

culations which were performed for the final energy prescription (FEP) and the initial energy prescription (IEP) are generally found to be insignificant. The calculations shown are for the FEP, except at $(-40°, 20°)$ where the results of both the FEP and the IEP are presented, since the largest difference between the two prescriptions is found here. The possible importance of off-shell effects in the evaluation of the two-body scattering in the DWIA formalism could serve as an explanation [6] for the discrepancy in the forward region. The only other significant discrepancy is at $(-40°, 70°)$. The reason for this is not obvious.

With regard to the choice of the specific optical-model potential used to generate distorted waves, the qualitative difference between the two sets of calculations is found to be relatively small. While the required normalization factors summarized in Table III indicate that the DWIA cross sections calculated with the Nadasen potentials overpredict the experimental results roughly by a factor of 2, the calculations based on the Madland potentials reproduce the experimental cross sections to within ~30%. This relatively large change in the absolute cross sections is probably related to modifications in the absorptive part of the central potential and to extrapolations of the optical potential to energies below 80 MeV and above 180 MeV which are the cutoff values for the range of validity of the Nadasen potentials.

The fact that the required normalization factors remain constant to within ~20% is a further indication of the consistency of the DWIA calculations in predicting quasifree knockout data. In contrast, previous studies [30, 31] on lighter targets yielded spectroscopic factors which increase with increasing scattering angle. These angle-dependent spectroscopic factors indicate inadequacies in the DWIA treatment. Whittal *et al.* [32], for example, relate the angle dependence of extracted spectroscopic factors to the inability of the DWIA to predict the high momentum components of the distorted momentum distribution. In these previous studies spectroscopic factors were obtained for single selected states, whereas in the present work the valence states were not resolved. The inadequacies of the DWIA description for a single momentum distribution might be obscured by the inclusion of the distorted momentum distributions for the other participating states, as the contribution from each state has a maximum at a different set of angles.

We conclude that the DWIA has the ability to predict quasifree ^{197}Au$(p, 2p)$ knockout cross sections consistently. The DWIA formalism, together with the relative occupation probabilities, was therefore assumed to be an appropriate description of the initial quasifree knockout process between the incoming proton and a bound valence nucleon in the continuum emission model.

B. Results for ^{197}Au$(p, p'p'')$

Before presenting the results of the complete calculation given by Eq. (7), we shall test the validity of the assumed reaction mechanism in a more intuitive, if less precise, way. It consists of simply overlaying the ^{197}Au$(p, p'p'')$ coincidence data with arbitrarily normalized inclusive ^{197}Au(p, p') spectra. This procedure has been successful in the previous studies [3, 6] on coincident continuum emission from ^{58}Ni and ^{12}C. It implies that, after the initial quasifree interaction, the struck nucleon interacts with the residual nucleus just as if it were an external projectile with an incident energy equal to that which was transferred to it in the quasifree interaction. If we assume that the major yield of quasifree knocked-out protons originates from valence states (say, up to a missing mass of 10 MeV as selected arbitrarily in our experiment), and that the residual target nucleus remains in the ground state with a negligible value of less than 1 MeV of the recoil energy, Eq. (3) reduces to

$$E_{a'} + E_b' = E_a + E_\lambda \ , \tag{8}$$

where E_λ corresponds to a proton binding energy of 10 MeV. The energy $E_{a'}$ of the quasifree proton which is detected as the primary proton $p_{a'}$, can thus be selected to give the required energy $E_b{}'$ of the struck proton, which is to be regarded as the subsequent "projectile" in the residual target. Appropriate energy cuts were performed around energy values of the primary proton of 90, 70, and 40 MeV, giving intranuclear projectile energies of 100, 120, and 150 MeV, respectively, which were specifically chosen to correspond to available inclusive ^{197}Au(p, p') data [27]. These cuts ranged ±8 MeV around the average values of 90 and 70 MeV and ±6 MeV for the average value of 40 MeV.

For the intercomparison of scattering angles between the coincident emission data and the inclusive data, we need to make a drastic assumption (which is not made in the complete calculation to follow), viz., that the yield of quasifree knocked-out particles is sufficiently peaked in a particular direction θ_b' (see Fig. 3) that it is meaningful to speak of an *average* angle θ_b'' between the "beam" of intranuclear projectiles and the angle at which the secondary proton is detected.

In Fig. 6, a set of continuum emission cross sections at a range of secondary proton emission angles θ_b has been overlayed with inclusive (p, p') spectra. The scattering angle $\theta_{p'}$ of the inclusive data (indicated in parentheses) has been chosen in each case to give the best match to the shape of the coincidence data. No emphasis is placed on the absolute magnitude of the spectra as the check merely indicates to what extent the coincidence cross sections are proportional to the inclusive data at the chosen scattering angles.

The significant result of this comparison is that the apparent direction Δ of the intranuclear projectile, i.e., the direction of the knocked-on proton, varies by no more than ±10° from the average direction indicated by $\bar{\Delta}$. This value is obtained by merely subtracting the inclusive scattering angle $\theta_{p'}$ from the detection angle of the secondary proton θ_b. The shape dependence of the energy distributions on the emission angle of coincident protons from the continuum is thus consistent with there being an initial quasifree interaction, followed by rescattering of the struck nucleon.

The results from this simple comparison of experimental spectra support the applicability of the proposed

model in the energy and angular range chosen for the continuum emission calculations of ^{197}Au$(p,p'p'')$. In order to perform the complete model calculation, DWIA cross sections were calculated to estimate the contribution of quasifree knocked-out protons and neutrons. In-plane proton and neutron distributions were obtained from the quasifree $(p,2p)$ and (p,pn) knockout reactions, and were calculated for three primary proton energies of 90, 70, and 40 MeV at two primary angles of $-40°$ and $-50°$.

Corresponding out-of-plane contributions were determined at the maximum secondary proton and neutron yields. Representative DWIA distributions which were calculated for primary protons of 90 MeV at an angle of $-40°$ are shown in Fig. 7. Spectroscopic factors of the relevant states were kept constant and correspond to the values which were required to fit the experimental cross sections for the discrete $(p,2p)$ knockout as described in the previous section. The almost equal strength of the calculated proton and neutron knockout yields illustrates the importance of including the contributions from neutron knockout in the assumed reaction mechanism as was also concluded by Pilcher *et al.* [6].

Complete calculations of the coincident continuum

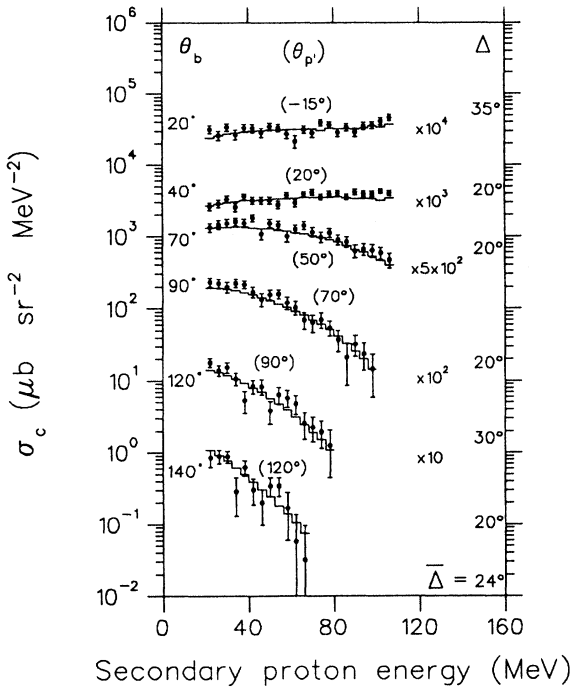

FIG. 6. Coincident continuum emission cross sections of the reaction ^{197}Au$(p,p'p'')$ at a primary proton energy of 70 MeV are shown at a primary scattering angle of $-40°$ as a function of the secondary proton energy at secondary scattering angles θ_b as indicated. Statistical error bars are shown with the experimental data. Arbitrarily normalized inclusive spectra of the reaction ^{197}Au(p,p') induced by 120 MeV protons at scattering angles indicated in parentheses are represented by the continuous curves. Differences between these angles and θ_b are listed under Δ. Note the displacement factors for the purpose of display.

emission cross sections, as expressed by the convolution integral in Eq. (7) for the reaction ^{197}Au$(p,p'p'')$ induced by 200 MeV protons, are displayed as solid curves together with the experimental measurements in Fig. 8. The calculations were normalized by a single factor κ for each set of data at a given primary energy $E_{a'}$ and angle $\theta_{a'}$.

The qualitative agreement between the model calculations and the experimental coincident cross sections is exceptionally good, considering the wide range of geometries covered. In general the shapes of the spectra are only weakly dependent on primary energy $E_{a'}$ and angle $\theta_{a'}$. For the forward secondary angles θ_b up to about 70°, the spectra all reveal rather flat cross sections except at the primary energy cut of 90 MeV. Here, the observed enhancement in the yields above a secondary proton energy of about 80 MeV measured at the secondary angles of 20° and 40° is likely to be due to contributions from collective states, which are not included in the theoretical model. As the detection angle of the secondary proton increases, all the energy distributions are characterized by an exponential falloff and a decrease of the absolute values. This feature is in agreement with the inclusive ^{197}Au(p,p') spectra measured at similar scattering angles and incident energies [27]. In the coincidence measurement, the dissipation of the projectile energy is however tracked explicitly. The theoretical treatment of this, i.e., folding the distribution of quasifree knocked-out nucleons with an expression for possible further rescattering of the struck nucleons off the residual nucleus, follows this trend remarkably well.

The model calculations indicate that the secondary angle range (20°–40°) accounts for the bulk of the measured coincident continuum yield, where contributions to the secondary proton channel from inelastic rescattering between the struck nucleon and the residual nucleus are assumed to be minimal. As the detection angle of the secondary proton increases to beyond this region, relatively more emitted protons will have been subjected to subsequent multiple scattering. The qualitative features of the spectra are found to be consistent with results which were obtained under similar experimental conditions for ^{58}Ni$(p,p'p'')$ by Ciangaru *et al.* [3] and ^{12}C$(p,p'p'')$ by Pilcher *et al.* [6].

However, the theoretical model underpredicts the coincident continuum emission cross sections severely. The normalization factors which were obtained are larger than those obtained in the above-mentioned studies [3, 6] on lighter systems. On the other hand, if the simplicity of the model is considered these results are not too surprising. Despite the inability of the coincident continuum emission model to reproduce the absolute cross sections satisfactorily, it clearly has the predictive power to describe the proposed reaction mechanism in terms of a simple convolution integral over a wide range of angles.

We have checked the accuracy of our assumption of a major in-plane contribution which scales down in phase space as a function of a relative out-of-plane distribution. For two specific cases, at primary energies of 90 and 40 MeV for a primary angle of $-40°$, the out-of-plane contributions were explicitly calculated, as in the analysis by

Pilcher *et al.* [6]. These more rigorous calculations change the normalization factors by 20% and 10%, respectively. Consequently, we are satisfied that our approach yields results which are within the expected uncertainty of the model.

The observed trend of increasing normalization factors with decreasing primary energy $E_{a'}$ has the following possible explanation. In the applied model, the description of the reaction is simplified by assuming that the projectile becomes the primary proton in the exit channel of the quasifree proton-nucleon doorway process. Although the DWIA predictions for discrete $(p, 2p)$ knockout have shown that the initial process of a quasifree proton-nucleon interaction can be applied with confidence over a wide angular range, the attenuation effect of the nuclear medium on the primary proton is restricted to the optical potential which generates the corresponding wave function. Additional inelastic scattering contributions to the primary proton channel are excluded from the model for the sake of simplicity. Ciangaru *et al.* [3] omitted the multiple scattering chain of the primary protons on the grounds of having selected relatively high-energy protons. The inclusion of data at relatively low primary energies (e.g., 40 MeV) in the present study therefore extrapolates this model to energies where multiple scattering can be expected to be important.

A further uncertainty in the calculated cross sections for coincident continuum emission which affects all the results is related to the treatment in the initial step of a quasifree neutron-knockout process and the subsequent inelastic (n, p) scattering. Although experimental (p, pn) cross sections have been interpreted successfully in terms of the DWIA [25] doubt has been expressed regarding the ability of the geometry-dependent hybrid (GDH) model [33] to predict absolute inelastic (n, p) cross sections for neutron energies above 100 MeV [34], which are required for the present analysis. However, the uncertainty affects only the angle-integrated cross section $\frac{d\sigma^{\text{inel}}}{dE_b}$ in Eq. (7), as the shape of the (n, p) angular distributions is determined from the more reliable Kalbach parametrization [26].

Despite the inability of the model to predict the absolute cross sections, which we believe to be mainly the result of excluding contributions from multiple scatterings to the primary proton yield, satisfactory shape agreement between the theoretical and experimental distribu-

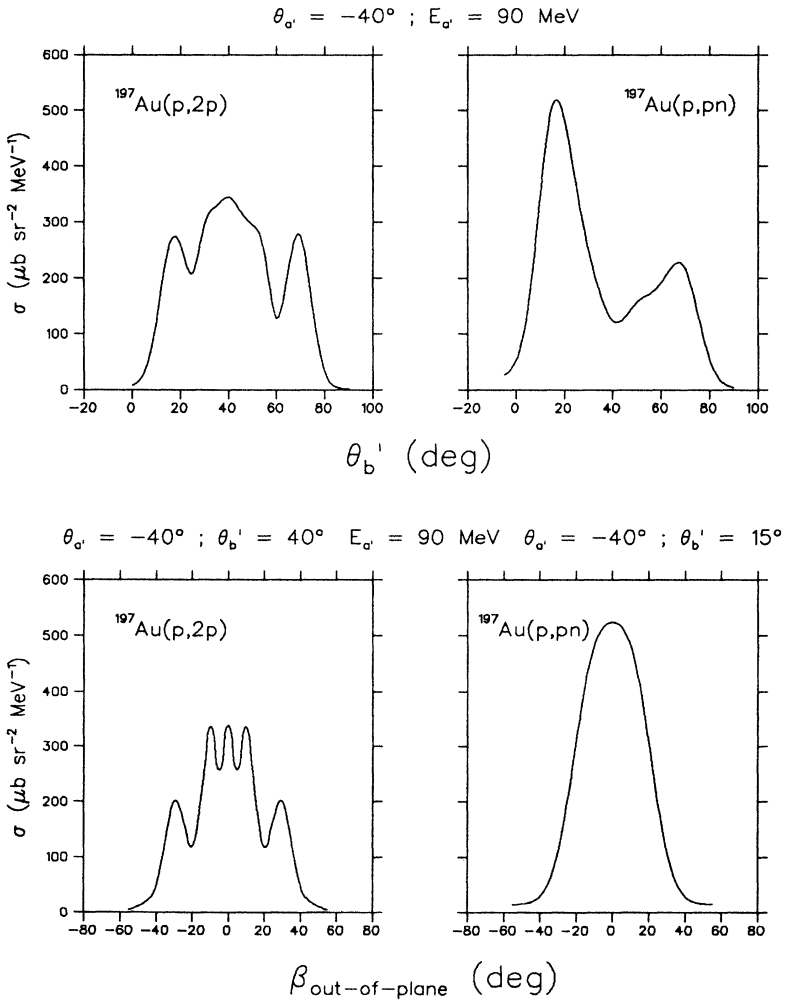

FIG. 7. A representative set of summed DWIA calculations of contributions from the ^{197}Au$(p, 2p)$ and ^{197}Au(p, pn) knockout reactions as a function of the in-plane (θ_b') and out-of-plane (β) scattering angle at an in-plane primary proton angle $\theta_{a'}$ of $-40°$ and energy $E_{a'}$ of 90 MeV. The out-of-plane angular distributions are shown at a secondary angle θ_b' where the in-plane knockout yield is a maximum.

tions has been found. These comparisons indicate that the quasifree scattering mechanism, which has been proposed to describe the initial process of a proton-induced coincident continuum reaction, plays a significant role in determining the correlations in energy and angle of the emitted particles. Although multiple scattering effects seem to play an increasingly important role as the selected primary proton energy decreases, they do not obscure the signature of quasifree knockout entirely, even in kinematic regions which do not favor such a mechanism. By relating the correlation between the two measured protons to the simplified continuum emission model of Ciangaru [4], we have shown that even for a nucleus as heavy as ^{197}Au the reaction mechanism for proton-

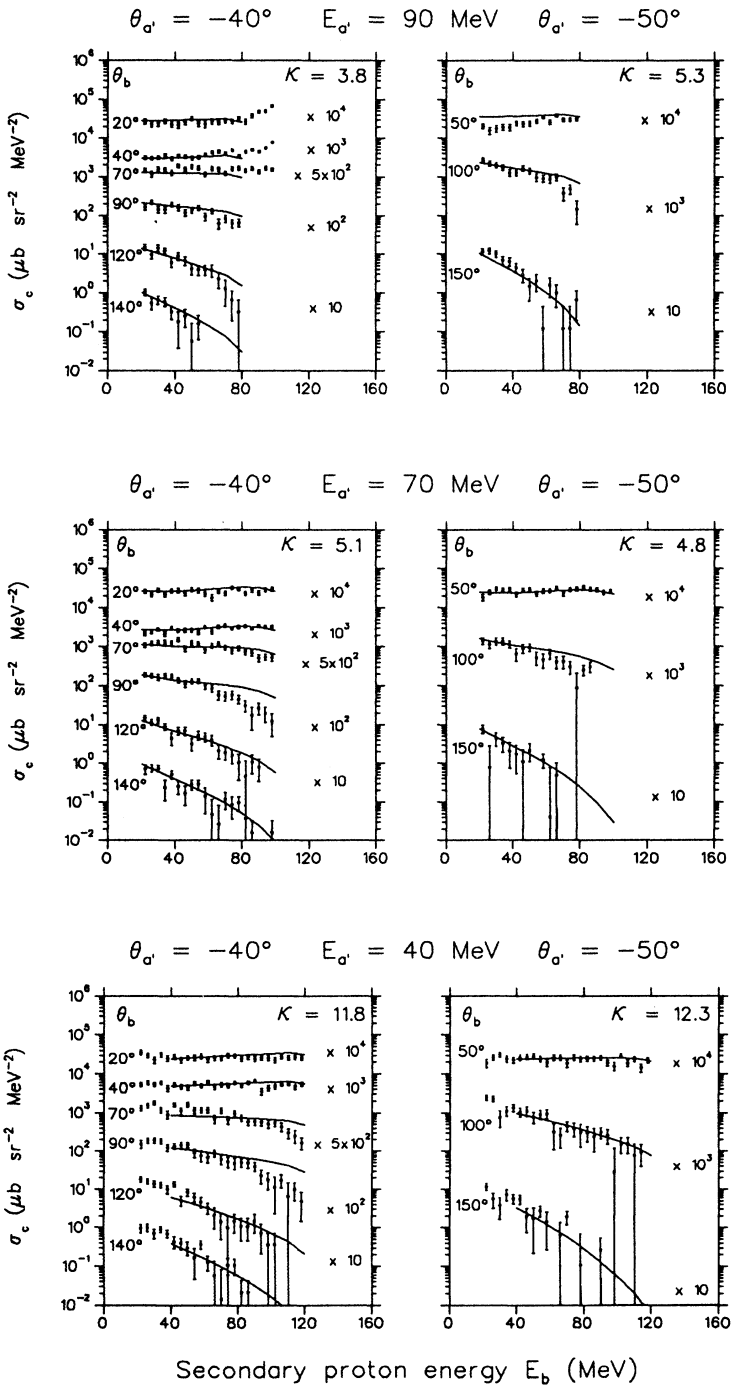

FIG. 8. Experimental coincident continuum emission cross sections for the reaction ^{197}Au$(p,p'p'')$ as a function of the secondary proton energy E_b and for coincidence angle pairs of the primary $(\theta_{a'})$ and the secondary (θ_b) scattering angles as indicated. Error bars represent the statistical error. The theoretical model calculations are given by the continuous curves which have been normalized by an amount κ for each set of primary energy and angle. Results have been multiplied by the indicated factors for the purpose of display.

induced continuum cross sections is dominated by the initial quasifree collision of the projectile with a valence nucleon.

VI. SUMMARY AND CONCLUSIONS

^{197}Au$(p,2p)$ and ^{197}Au$(p,p'p'')$ coincidence cross sections induced by 200 MeV protons were measured. The former notation refers to quasifree knockout, and the latter refers to coincident emission involving larger missing mass (assumed to arise from an initial quasifree interaction, followed by inelastic rescattering). In the analysis of the ^{197}Au$(p,2p)^{196}$Pt data, all those events were selected which mainly originate from the quasifree knockout of bound protons to experimentally unresolved discrete states of ^{196}Pt up to a missing mass of 10 MeV. Quasifree knockout contributions from the $1h_{11/2}$, $3s_{1/2}$, $2d_{3/2}$, and $2d_{5/2}$ proton orbitals were added incoherently in the DWIA calculations. The ratio of spectroscopic factors used to sum the calculated cross sections was chosen to be consistent with the occupation probabilities of these states as found by Langevin-Joliot *et al.* [24] except for the occupation probability of the $3s_{1/2}$ state which had to be increased to account for missing strength at the quasifree angles of $(-40°, 40°)$.

We found no significant effects relating to inadequacies of the on-shell approximation [15] for two-body scattering in the DWIA treatment. The DWIA reproduces the experimental discrete knockout distributions reasonably well but overpredicts the absolute magnitude of the cross sections by a factor of $\sim$2 based on an average occupation probability of $\sim$80% as suggested by Langevin-Joliot *et al.* [24]. This trend in the spectroscopic factors is in line with related DWIA calculations which have been performed by Samanta *et al.* [35] for ^{40}Ca$(p,2p)^{39}$K and by Cowley *et al.* [36] for ^{12}C$(p,2p)^{11}$B. Consequently, the DWIA theory may be used with confidence to model the quasifree doorway process in the continuum emission of ^{197}Au$(p,p'p'')$.

Cross sections for ^{197}Au$(p,p'p'')$ were interpreted in terms of a model described by Ciangaru [4], which has been tested in a simplified form in other studies [3, 6] by expressing the cross section as a convolution integral of a quasifree knockout distribution and the cross section for the inelastic interaction between the struck nucleon and the residual nucleus. As previously found [6] for ^{12}C$(p,p'p'')$, the contribution to the coincident continuum proton yield induced by a knocked-on neutron in the initial interaction, was shown to be significant. Uncertainties in the required theoretical predictions of neutron-induced proton emission could be reduced with the measurement of inclusive (n,p) and (p,n) data together with exclusive (p,pn) data on neutron-rich targets, which do not presently exist at these energies.

Although the calculations had to be normalized, their shape agreement with the experimental cross sections is acceptable throughout. These normalizations are much larger than were found in similar studies at an incident energy of 200 MeV for ^{58}Ni$(p,p'p'')$ [3] and ^{12}C$(p,p'p'')$ [6]. A possible explanation could be that any contributions to the continuum yield from multiple scattering of the *primary* protons inside the residual nucleus following the initial quasifree knockout process, are excluded from our version of the continuum emission model. While the values of the normalization factors remain almost constant with primary and secondary angles at the primary proton energies of 70 and 90 MeV, an increase of these values is found for a primary energy of 40 MeV. Although there are doubts about the validity of the continuum emission model when the primary proton is detected with a low kinetic energy, it has been shown that the model of Ciangaru [4] is generally applicable to ^{197}Au$(p,p'p'')$.

The inferred importance of a single proton-nucleon collision in the interaction of a 200 MeV proton with nuclear matter, with a relatively high probability of both partners in the collision emerging from the nucleus, supports the conclusions of the recent $(e,e'p)$ measurement of Garino *et al.* [37]. Their results imply a significantly longer mean-free path than previous calculations based on the free N-N cross section had suggested.

The present study has therefore demonstrated that interpretations and conclusions regarding the reaction mechanism of preequilibrium reactions drawn from the analysis of inclusive spectra alone, cannot necessarily be regarded as a complete approach to understanding the underlying physics. The quasifree scattering mechanism has often been discarded in models describing the formation process of the continuum on the grounds of the absence of clear signatures in the spectra of heavier nuclei (e.g., Refs. [38, 39]). Multistep direct [40–42] and single-step [43, 44] calculations have indicated however that an appreciable amount of the continuum emission originates from the first step. Although the aforementioned studies neglect contributions from two-particle emission, this study nevertheless illustrates the importance of a three-body breakup process at an incident energy of 200 MeV. By folding the single step of quasifree knockout with the subsequent stages of energy dissipation in the target nucleus, a relatively simple model qualitatively reproduces the coincident proton cross sections.

For quantum-mechanical multistep direct theories, the present study emphasizes the desirability of extending the expression of the first step to account for contributions from two-particle emission which result from a quasifree knockout process. A further challenge for these theories would then be to reproduce exclusive spectra which have been used in the present study, to confirm the role of an initial quasifree knockout process as a precursor to the emission of preequilibrium particles above the threshold of a three-body breakup process.

We thank C. J. Stevens and V. C. Wikner for their assistance.

[1] E. Gadioli and P. E. Hodgson, *Pre-Equilibrium Nuclear Reactions* (Oxford University Press, New York, 1992).
[2] A. A. Cowley, C. C. Chang, H. D. Holmgren, J. D. Silk, D. L. Hendrie, R. W. Koontz, P. G. Roos, C. Samanta, and J. R. Wu, Phys. Rev. Lett. **45**, 1930 (1980).
[3] G. Ciangaru, C. C. Chang, H. D. Holmgren, A. Nadasen, and P. G. Roos, Phys. Rev. C **29**, 1289 (1984).
[4] G. Ciangaru, Phys. Rev. C **30**, 479 (1984).
[5] Herman Feshbach, Arthur Kerman, and Steven Koonin, Ann. Phys. (N.Y.) **125**, 429 (1980).
[6] J. V. Pilcher, A. A. Cowley, D. M. Whittal, and J. J. Lawrie, Phys. Rev. C **40**, 1937 (1989).
[7] A. A. Cowley, S. V. Förtsch, J. J. Lawrie, J. V. Pilcher, F. D. Smit, and D. M. Whittal, Europhys. Lett. **13**, 37 (1990).
[8] R. E. L. Green, D. H. Boal, R. L. Helmer, K. P. Jackson, and R. G. Korteling, Nucl. Phys. **A405**, 463 (1983).
[9] D. F. Measday and C. Richard-Serre, Nucl. Instrum. Methods **76**, 45 (1969).
[10] Joseph F. Janni, At. Data Nucl. Data Tables **27**, 147 (1982).
[11] N. S. Chant, Code THREEDEE, University of Maryland (unpublished).
[12] N. S. Chant and P. G. Roos, Phys. Rev. C **15**, 57 (1977).
[13] N. S. Chant, P. Kitching, P. G. Roos, and L. Antonuk, Phys. Rev. Lett. **43**, 495 (1979).
[14] N. S. Chant and P. G. Roos, Phys. Rev. C **27**, 1060 (1983).
[15] Edward F. Redish, G. J. Stephenson, Jr., and Gerald M. Lerner, Phys. Rev. C **2**, 1665 (1970).
[16] F. A. Brieva and W. G. Love, Phys. Rev. C **42**, 2573 (1990).
[17] Yoshiteru Kudo, Noriyo Kanayama, and Takashi Wakasugi, Phys. Rev. C **38**, 1126 (1988).
[18] Yoshiteru Kudo, Noriyo Kanayama, and Takashi Wakasugi, Phys. Rev. C **39**, 1162 (1989).
[19] A. A. Cowley, J. V. Pilcher, J. J. Lawrie, and D. M. Whittal, Phys. Lett. B **201**, 196 (1988).
[20] A. Nadasen, P. Schwandt, P. P. Singh, W. W. Jacobs, A. D. Bacher, P. T. Debevec, M. D. Kaitchuck, and J. T. Meek, Phys. Rev. C **23**, 1023 (1981).
[21] David G. Madland, Los Alamos National Laboratory Report LA–UR–87–3382.
[22] P. Schwandt, H. O. Meyer, W. W. Jacobs, A. D. Bacher, S. E. Vigdor, M. D. Kaitchuck, and T. R. Donoghue, Phys. Rev. C **26**, 55 (1982).
[23] K. A. Keller, J. Lange, and H. Münzel, in *Numerical Data and Functional Relationships in Science and Technology*, edited by K.-H. Hellwege (Springer-Verlag, Berlin, 1973), Vol. 5, Part A, pp. 8, 10, and 13.
[24] H. Langevin-Joliot, E. Gerlic, J. Guillot, J. van de Wiele, S. Y. van der Werf, and N. Blasi, Nucl. Phys. **A462**, 221 (1987).
[25] J. W. Watson, M. Ahmad, D. W. Devins, B. S. Flanders, D. L. Friesel, N. S. Chant, P. G. Roos, and J. Wastell, Phys. Rev. C **26**, 961 (1982).
[26] C. Kalbach, Phys. Rev. C **37**, 2350 (1988).
[27] A. A. Cowley, S. V. Förtsch, J. J. Lawrie, D. M. Whittal, F. D. Smit, and J. V. Pilcher, Z. Phys. A **336**, 189 (1990).
[28] M. Blann, Code ALICE/85/300, Lawrence Livermore National Laboratory Report No. UCID–20169, 1984 (unpublished).
[29] R. Silberberg and C. H. Tsao, Phys. Rep. **191**, 351 (1990).
[30] J. S. Wesick, P. G. Roos, N. S. Chant, C. C. Chang, A. Nadasen, L. Rees, N. R. Yoder, A. A. Cowley, S. J. Mills, and W. W. Jacobs, Phys. Rev. C **32**, 1474 (1985).
[31] S. V. Förtsch, A. A. Cowley, J. V. Pilcher, D. M. Whittal, J. J. Lawrie, J. C. van Staden, and E. Friedland, Nucl. Phys. **A485**, 258 (1988).
[32] D. M. Whittal, A. A. Cowley, J. V. Pilcher, S. V. Förtsch, F. D. Smit, and J. J. Lawrie, Phys. Rev. C **42**, 309 (1990).
[33] M. Blann and H. K. Vonach, Phys. Rev. C **28**, 1475 (1983).
[34] W. Scobel, M. Trabandt, M. Blann, B. A. Pohl, B. R. Remington, R. C. Byrd, C. C. Foster, R. Bonetti, C. Chiesa, and S. M. Grimes, Phys. Rev. C **41**, 2010 (1990).
[35] C. Samanta, N. S. Chant, P. G. Roos, A. Nadasen, J. Wesick, and A. A. Cowley, Phys. Rev. C **34**, 1610 (1986).
[36] A. A. Cowley, J. V. Pilcher, J. J. Lawrie, and D. M. Whittal, Phys. Rev. C **40**, 1950 (1989).
[37] G. Garino *et al.*, Phys. Rev. C **45**, 780 (1992).
[38] H. Machner, D. Protić, G. Riepe, J. P. Didelez, N. Frascaria, E. Gerlic, E. Hourani, and M. Morlet, Phys. Lett. **138B**, 39 (1984).
[39] R. E. Segel, S. M. Levenson, P. Zupranski, A. A. Hassan, S. Mukhopadhyay, and J. V. Maher, Phys. Rev. C **32**, 721 (1985).
[40] A. A. Cowley, A. van Kent, J. J. Lawrie, S. V. Förtsch, D. M. Whittal, J. V. Pilcher, F. D. Smit, W. A. Richter, R. Lindsay, I. J. van Heerden, R. Bonetti, and P. E. Hodgson, Phys. Rev. C **43**, 678 (1991).
[41] A. J. Koning and J. M. Akkermans, in *Proceedings of the International Conference on Nuclear Data for Science and Technology, Jülich, 1991*, edited by S. M. Qaim (Springer-Verlag, Berlin, 1992), p. 891.
[42] W. A. Richter, A. A. Cowley, R. Lindsay, J. J. Lawrie, S. V. Förtsch, J. V. Pilcher, R. Bonetti, and P. E. Hodgson, Phys. Rev. C **46**, 1030 (1992).
[43] G. F. Bertsch and O. Scholten, Phys. Rev. C **25**, 804 (1982).
[44] Y. L. Luo and M. Kawai, Phys. Rev. C **43**, 2367 (1991).